

CHAPTER 4

Synthesis and Characterization of 'Whiskers'

This chapter attempts to determine the experimental parameters and conditions of the synthesis of alumina borate whiskers by first mixing the water-soluble starting materials in deionized water. Alumina borate ($\text{Al}_{18}\text{B}_4\text{O}_{33}$) whiskers are gaining their applications as reinforcements in metal matrix composite and oxidation-resistant composite fabrication due to their high surface to volume ratio, high melting point, low coefficient of thermal expansion ($4.2 \times 10^{-6} \text{ }^\circ\text{C}^{-1}$), high young's modulus (8 GPa) [86-90]. Apart from these, the cost of this whisker is low as compared to other ceramic whiskers. Aluminium borate whiskers have been synthesized by hydrolysis route using alumina (Al_2O_3) and boric acid. The effect of sintering temperature was studied in the range of 950 to 1400 $^\circ\text{C}$ on the formation of microstructures and the associated mechanical strength of the synthesized whiskers. Processes to synthesize alumina borate whiskers involve high processing temperature, high energy consumption, and reaction catalysts [91-95]. The hydrolyzation route has several unique advantages like low processing temperature, simple technique to control the shape and size of materials, and involved low process cost without using a catalyst and costly precursors. In this chapter microstructural evolution has been characterized using differential thermal analysis (DTA-TGA), x-ray diffraction analysis (XRD), scanning electron microscopy with energy dispersive spectroscopy (EDS), and transmission electron microscopy was utilized to ascertain the formation of whiskers. The result have been discussed comprehensively based on observation made during the characterization.

4.1 Morphological study of reinforcing whiskers

The SEM images of whisker growth taken place in samples during sintering in the temperature range of 950-1400°C for 4 hours are shown in **Figure 4.1**. The sample sintered at 950 °C, shows mainly the $\text{Al}_4\text{B}_2\text{O}_9$ phase **Figure 4.1(a)**. While samples sintered at 1100 °C show small whiskers of the $\text{Al}_{18}\text{B}_4\text{O}_{33}$ phase in **Figure 4.1 (b&c)**.

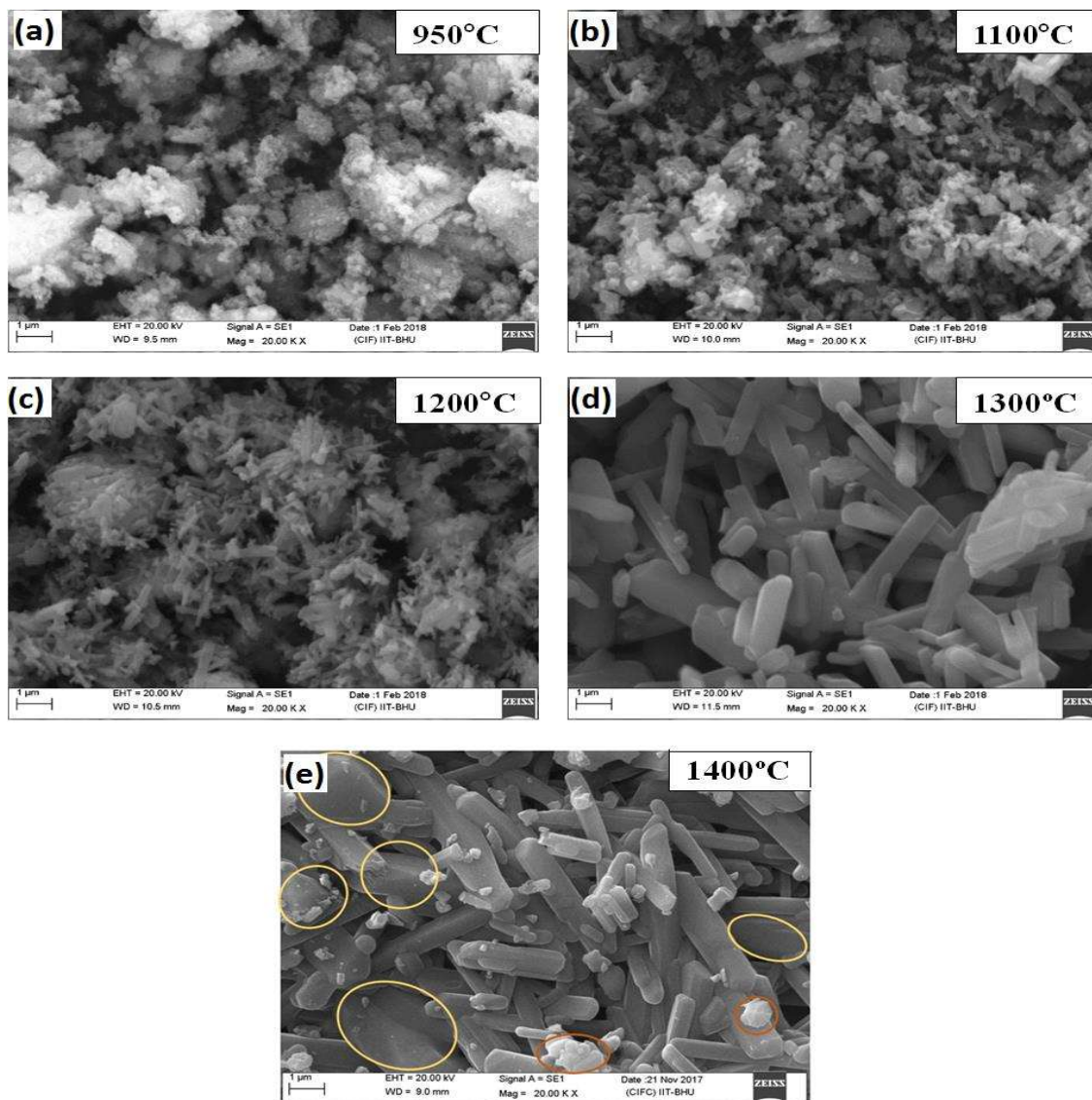


Figure 4.1: SEM micrographs of samples sintered at (a) 950 °C, (b) 1100 °C, (c) 1200 °C, (d) 1300 °C and (e) 1400 °C. Encircled area in 1400 °C sample shows agglomerate formation and melting of whiskers

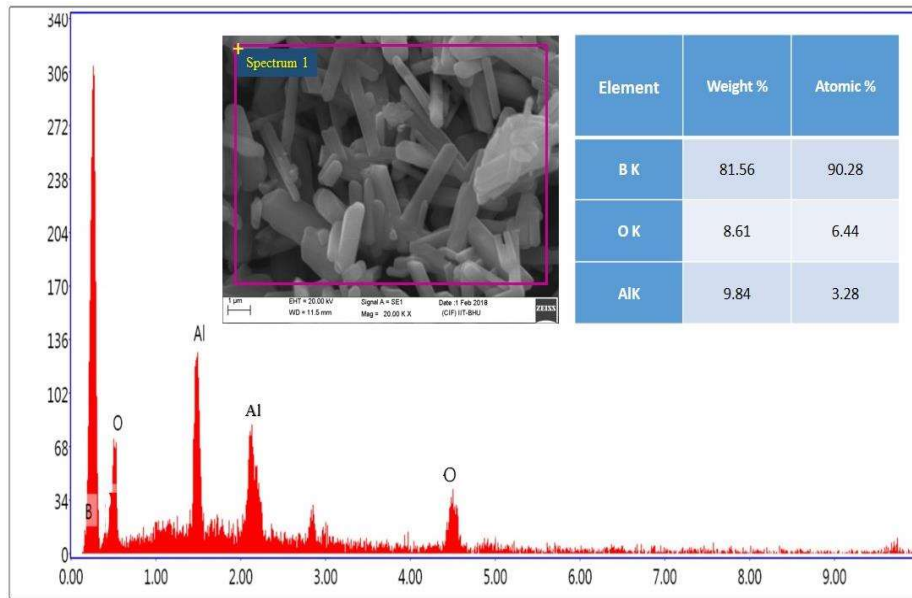


Figure 4.2: EDAX of sample sintered at 1300 °C

The corresponding EDAX analysis in **Figure 4.2** shows the presence of Al, B, and O in the samples. EDAX has been carried out to analyze each element present in the bulk material and the weight percentage of particular elements at a specific region was observed.

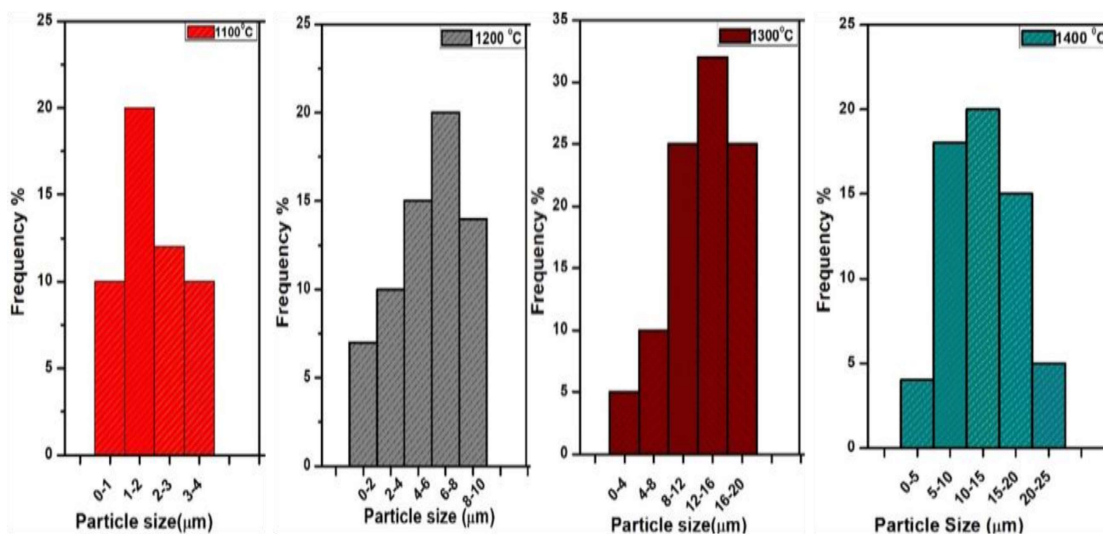


Figure 4.3: Average particle length at various sintering temperatures

The particle size distribution at different sintering temperatures is shown in **Figure 4.3**. Particle size distribution was measured using the absolute measurement method by SEM micrograph in which particle size is measured directly from micrograph and the mean of the largest dimension of particles was considered particle size. At 1100 °C, high volume fractions of particle size of 1-2 μm are observed. As the sintering temperature is increased to 1200 °C, the particle size range has been increased (6-8 μm). Further, at a higher sintering temperature of 1300 °C, the particle size of whiskers 10-15 μm are observed, resulting in an improvement in the length of whiskers. A non-uniform particle size at 1400 °C shows a decline in whisker growth with increasing sintering temperature and the formation and melting of whiskers.

As the soaking period is increased, the diameter of the whiskers at various temperatures varied in the range of 0.2-1 μm, showing an increase in aspect ratio (maximum 20:1) with an increase in temperature upto 1300 °C.

The XRD patterns of samples sintered in the range of 950-1400 °C are shown in **Figure 4.4**, referring to JCPDS (47-0319) and JCPDS (32-0003) for Al₄B₂O₉ and Al₁₈B₄O₃₃ respectively. The XRD pattern of the sample sintered at 950 °C shown the presence of two phases such as Al₄B₂O₉ and Al₁₈B₄O₃₃ in **Figure 4.4 (a)**. The XRD profile corresponding to 1100 °C in **Figure 4.4 (b)** shows Al₁₈B₄O₃₃ as the majority phase [86]. This increasing trend is followed at 1200°C and 1300°C in **Figure 4.4 (c&d)**. Samples sintered at 1400 °C presented only one of the phases (Al₁₈B₄O₃₃) with smaller peaks. These minor peaks represent a decrease in crystalline phase.

The morphological and discontinuous structure of the micro rods (whiskers) was characterized by transmission electron microscopy, and the crystal parameters are determined as a=7.6874 Å, b=15.0127 Å, and c=5.6643 Å. The parameters confirm the

orthorhombic $\text{Al}_{18}\text{B}_4\text{O}_{33}$ phase. Bright-field images with corresponding diffraction patterns of these samples have been shown in **Figure 4.5**. The average length of micro rods in this phase was found to be 10-15 μm . The micro rods were crystallized well, as can be seen from TEM images. **Figure 4.5 (a)** shows the representative TEM image of a single crystal of $\text{Al}_{18}\text{B}_4\text{O}_{33}$ observed in a sample sintered at 1300 $^{\circ}\text{C}$.

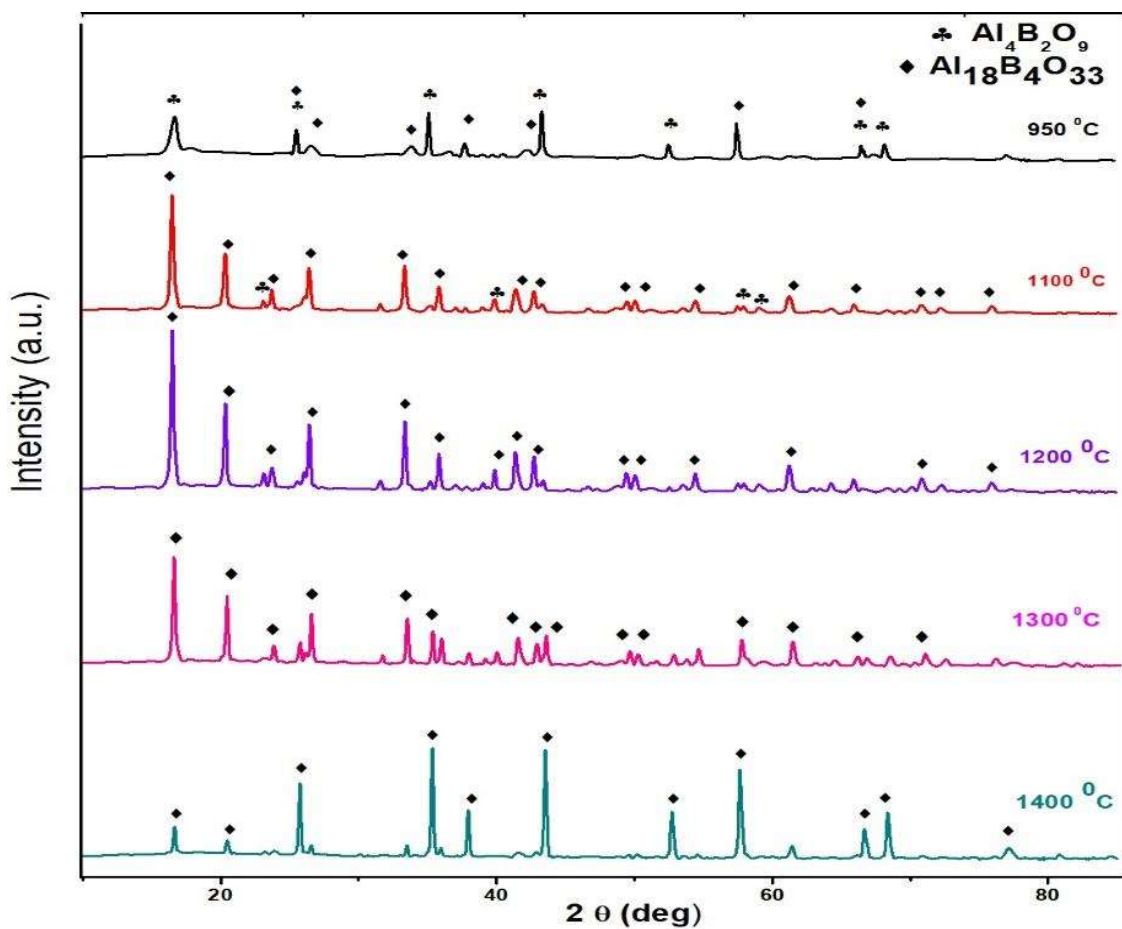


Figure 4.4: XRD patterns of samples sintered at (a) 950 $^{\circ}\text{C}$, (b) 1100 $^{\circ}\text{C}$, (c) 1200 $^{\circ}\text{C}$, (d) 1300 $^{\circ}\text{C}$, and (e) 1400 $^{\circ}\text{C}$

The selected area electron diffraction (SAED) pattern acquired in the $[210]$ -axis zone shown in **Figure 4.5 (b)** indicates that the whisker is single-crystalline. **Figure 4.5 (c)** shows a representative TEM micrograph of the sample sintered at 1400 $^{\circ}\text{C}$.

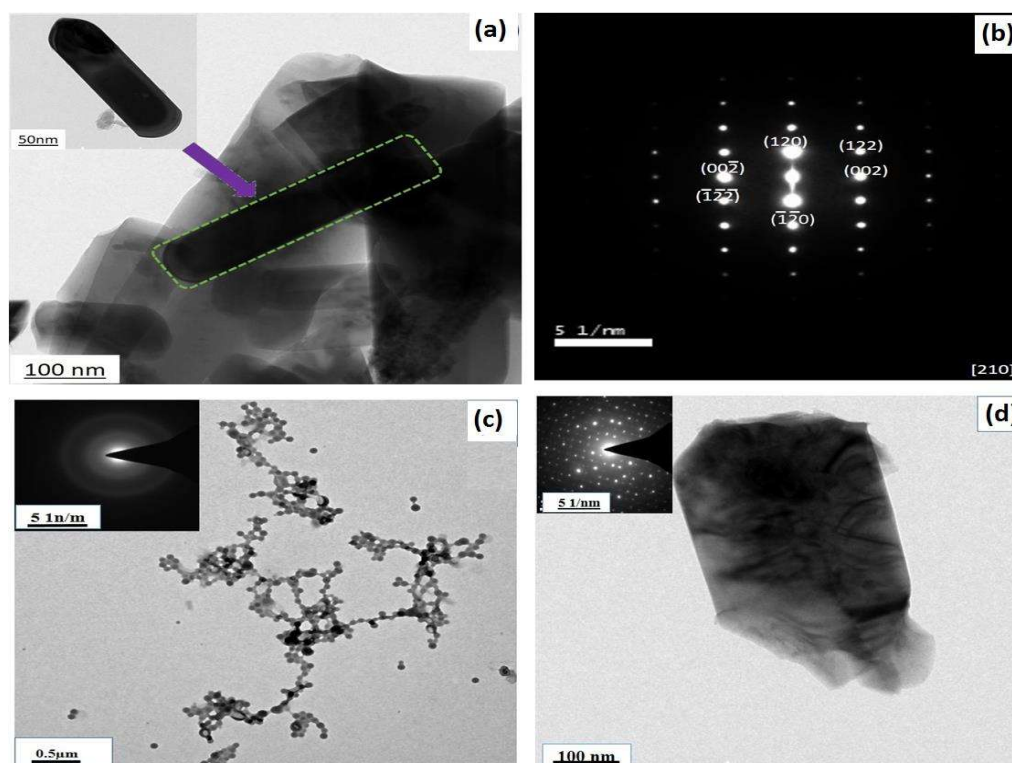


Figure 4.5: (a) Bright field Image (b) corresponding SAED of ABO_w powder sintered at $1300\text{ }^\circ\text{C}$ (c) Bright-field image and corresponding SAED (inset) of a network of ABO_w powder sintered at $1400\text{ }^\circ\text{C}$ (d) magnified bright field image of particle from fig.4.5c and corresponding SAED (inset)

From the corresponding bright-field images, it is clear that network formation of whiskers has taken place. The magnified image of the particle shown from bright-field image (4.5c) of the network area shows that the aspect ratio of whiskers starts decreasing, as shown in Figure 4.5 (d). Diffraction patterns are not similar to the sample sintered at 1300°C , but they are random spots. So it can be concluded these are not a single crystal.

4.2. Physical properties (density/Porosity) of sintered samples

The physical properties viz. bulk density and apparent porosity of sintered samples are shown in Table 4.1. It is evident from Table 4.1 that the bulk density of

samples decreased up to 1300°C and increased again at 1400°C. The decrease in bulk densities may result from the formation of needle-like sharp microstructures with increasing sintering temperatures. At 1400°C, an increase in density may be the result of network formation from whiskers; this may also be confirmed for SEM structures that show deformation of needle-like whiskers similarly apparent porosity increases up to 1300 °C and decreases at 1400 °C.

Table 4.1: Physical properties (density/porosity) of samples-

| Sample | Sintering temperature (°C) | Bulk density (g /cc) | Apparent Porosity (%) |
|---------------|-----------------------------------|-----------------------------|------------------------------|
| 1 | 950 | 1.82 | 15.6 |
| 2 | 1100 | 1.72 | 32.4 |
| 3 | 1200 | 1.68 | 38.5 |
| 4 | 1300 | 1.64 | 39.3 |
| 5 | 1400 | 1.77 | 33.8 |

The sample sintered at 950°C shows minimum % porosity. As whiskers formation increases with an increase in sintering temperature, the % porosity increases due to an increase in the generated void spaces between the whiskers. At 1400 °C, agglomerate formation due to the melting of whiskers can cause a decrease in void spaces leading to a decrease in % porosity. Thus the study of density and porosity

behavior of whiskers shows to formulating the sintering temperature 1300 °C for the preparation of whiskers.

4.3. Thermal analysis

Figure 4.6 shows the DTA and TG analysis of powdered samples. Weight loss and negligible weight change are observed in the whole thermal study. In DTA curves, decomposition of H_3BO_3 can be observed. The crest at 180°C is due to an endothermic reaction while dehydration of boric acid.

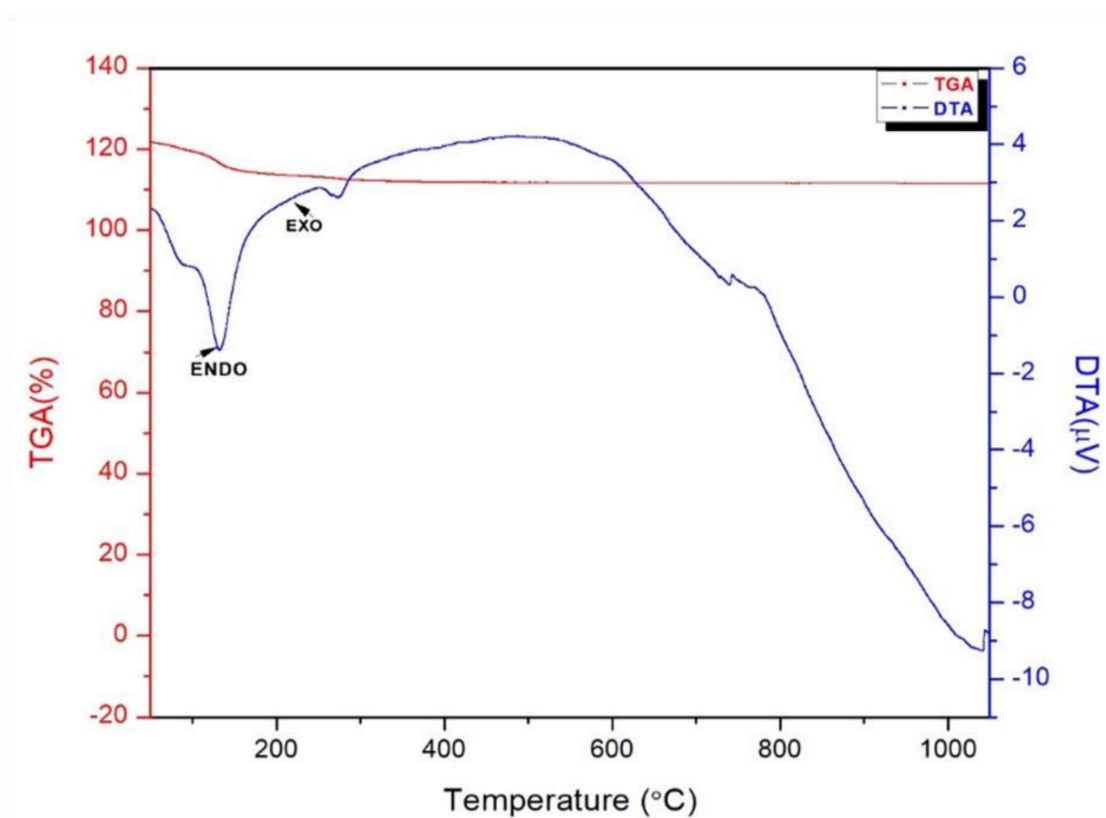


Figure 4.6: DSC and TG curves of alumina borate mixture

No reaction takes place between B_2O_3 and Al_2O_3 below 700°C. Initiation of $2Al_2O_3 \cdot B_2O_3$ phase formation takes place between 700-800 °C, which reacts with excess alumina above 950°C, giving the $Al_{18}B_4O_{33}$ phase. The reaction was found to be

completed at 1100 °C. Nucleation and growth of whiskers led to slowing down of endothermic trend. TGA curve shows a weight loss of 3-4 %, which is attributed to the decomposition of H_3BO_3 to B_2O_3 . These phases undergo polymorphic reversible or irreversible transitions over the temperature range between 350-800 °C. Above 350 °C, no weight loss was observed.

4.4 Flexural strength analysis

Table 4.2 shows the modulus of rupture (flexural strength) values at room temperature and 700 °C for different sintering temperatures. At room temperature test is called CMOR (cold modulus of rupture), and the high-temperature test is called HMOR (hot modulus of rupture) [96-97].

Table 4.2: CMOR and HMOR of sintered samples

| Sintering temperature (°C) | Cold Modulus of Rupture at room temperature (MPa) | Hot Modulus of Rupture at 700 °C (MPa) |
|----------------------------|---|--|
| 950 | 11 ± 3 | 9 ± 3 |
| 1100 | 29 ± 3 | 22 ± 3 |
| 1200 | 42 ± 3 | 34 ± 3 |
| 1300 | 51 ± 3 | 42 ± 3 |
| 1400 | 45 ± 3 | 39 ± 3 |

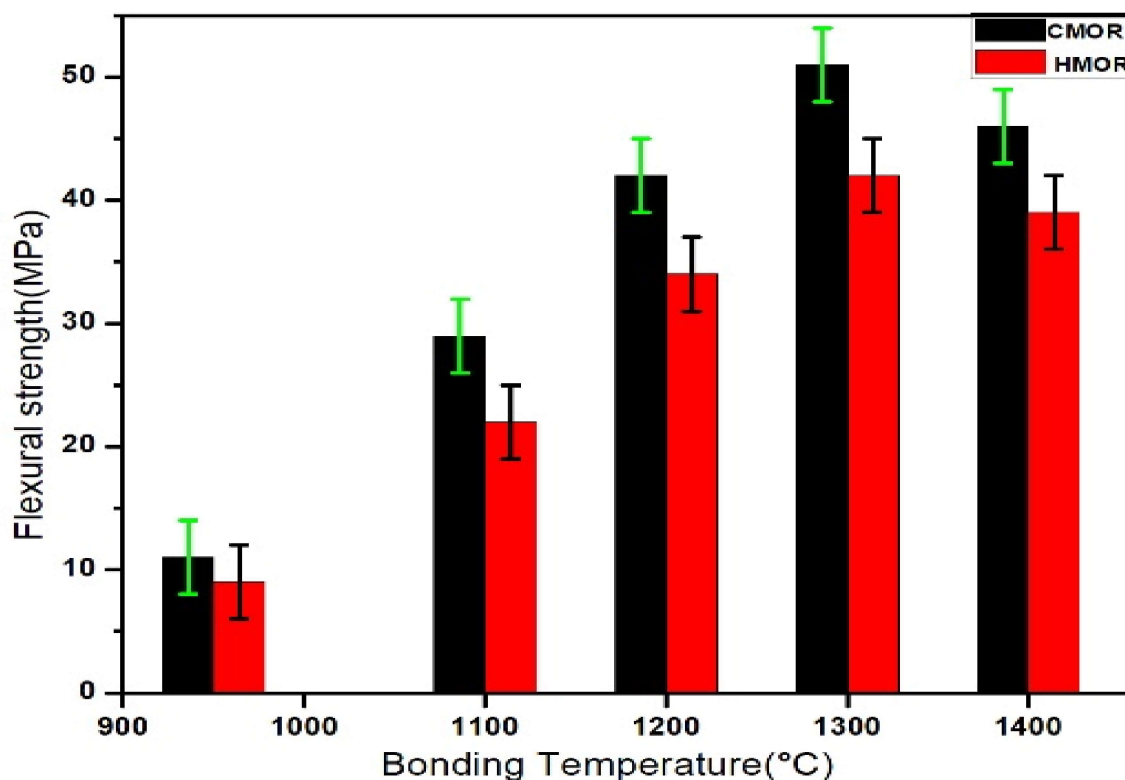


Figure 4.7: Room temperature and high temperature (700°C) flexural strength with corresponding bonding temperature

The values for CMOR and HMOR were observed to be increasing for samples sintered up to 1300 °C due to successive sintering processes and increasing bonding strength. Samples sintered at 1200 °C show higher values than samples at 950 °C and 1100 °C, as whisker formation starts after 1100 °C, as shown in **Figure 4.7**. However, values decreased for the sample sintered at 1400 °C, perhaps due to the initiation of formation of brittle, glassy phase. As expected, for samples, HMOR values are also lower than CMOR values due to high thermal stresses leading to plastic deformation. The above analysis shows that the HMOR values for samples improved up to 42 MPa at 700 °C.

4.5 Chapter summary

The above analysis investigated the effect of varying sintering temperatures on alumina borate materials obtained by following a low-cost hydrolysis route. Thermal analysis following DTA and TGA shows that $\text{Al}_{18}\text{B}_4\text{O}_{33}$ phase initiates above 950°C and completes at 1100°C . The apparent porosity of samples increases with increasing sintering temperature but drops sharply after 1300°C . XRD confirmed the presence of the $\text{Al}_{18}\text{B}_4\text{O}_{33}$ phase, which is crystalline between 1200 - 1300°C . TEM investigation shows the micro rods observed in the $\text{Al}_{18}\text{B}_4\text{O}_{33}$ phase were single crystals with orthorhombic structures. But TEM analysis of sample sintered at 1400°C shows the crystals start to form a network thus confirming the melting of whiskers at higher temperatures. SEM images show the size of whiskers (micro rods) increase with an increase in temperature up to 1300°C (10 - $15\mu\text{m}$), but an increase in temperature further led to a decrease in the length of the crystals. The thermo-mechanical behavior of the samples shows the modulus of rupture is higher at room temperature than those at 700°C . It clearly shows the increase in temperature leads to weak mechanical behavior of alumina borate whiskers. The strength at this elevated temperature is relatively high for further use as reinforcement in metal matrix composites.

